~~Simulated Idealized Arctic Cloud Sensitivity to~~ Above Cloud CCN Concentrations Help to Sustain Some Arctic Low-Level Clouds

Lucas J. Sterzinger[1,2,3] and Adele L. Igel[1]

[1]Department of Land, Air and Water Resources, University of California, Davis, Davis, California, USA
[2]NASA Goddard Space Flight Center, Greenbelt, Maryland, USA
[3]ADNET Systems, Inc, Bethesda, Maryland, USA

Correspondence: Adele L. Igel (aigel@ucdavis.edu)

Abstract. ~~Recent studies have reported observations of enhanced aerosol concentrations directly above the Arctic boundary layer, and it has been suggested that Arctic boundary layer clouds could entrain these aerosol and activate them~~Previous studies have found that low-level Arctic clouds often persist for long periods even in the face of very low surface cloud condensation nuclei (CCN) concentrations. Here we investigate whether these conditions could occur due continuous entrainment of aerosol particles from the free troposphere. We use an idealized LES modeling framework where aerosol concentrations are ~~kept~~ low in the boundary layer, ~~and~~ but increased up to 50x in the free troposphere. We find that the ~~simulations~~ tests with higher tropospheric aerosol concentrations simulated clouds which persisted for longer and ~~had~~ maintained higher liquid water ~~path~~paths. This is due to direct entrainment of the tropospheric aerosol into the cloud layer which results in a precipitation suppression from the increase in cloud droplet number and in stronger ~~radiative cooling at cloud top due to the higher liquid water content at cloud top~~cloud top radiative cooling, which causes stronger circulations maintaining the cloud in the absence of surface forcing. Together, these two responses result in a more well-mixed boundary layer with a top that ~~does not move rapidly in time such that it~~ remains in contact with the tropospheric aerosol reservoir and can maintain entrainment of those aerosol particles. The ~~boundary layer aerosol and cloud droplet~~ surface aerosol concentrations, however, remained low in all simulations. ~~Surface based measurements in this case would not necessarily suggest the influence of tropospheric aerosol on the cloud, despite it being necessary for stable cloud persistence.~~ The free tropospheric aerosol concentration necessary to maintain the clouds is consistent with concentrations that are frequently seen in observations.

1 Introduction

~~The Arctic is now estimated to be warming at four times the global mean warming rate (Rantanen et al., 2022). Clouds play a large role in this amplification, with the net cloud feedback in the Arctic estimated to be +0.58 K with a doubling of CO_2, which contributes to 15% of the warming in the Arctic in such a scenario (Taylor et al., 2013).~~ Low level mixed-phase clouds are crucial regulators of Arctic climate (Intrieri et al., 2002; Shupe and Intrieri, 2004; Sedlar et al., 2011) and are ubiquitous (Shupe et al., 2006, 2011; Shupe, 2011). ~~These clouds' precise radiative forcing at the surface is not well quantified; for a majority of the year they exert a warming effect on the surface due to the high albedo of an ice surface and limited solar radiation (Shupe and Intrieri, 2004; Sedlar et al., 2011). During the late summer, however, the clouds can have a cooling effect~~

~~as surface albedo decreases due to melting ice and solar insolation increases.~~ Properly modeling these clouds is ~~crucial to accurately projecting~~ necessary to accurately project Arctic and global climate change, yet representation of Arctic low-level clouds in models has remained a challenge. (Klein et al., 2009; Morrison et al., 2009, 2011, 2012; Sotiropoulou et al., 2016).

Low-level Arctic clouds have been observed to exist for days at a time (Shupe, 2011; Shupe et al., 2011; Morrison et al., 2012; Verlinde et al., 2007). This is especially curious given the low aerosol concentrations in the Arctic; boundary layer aerosol concentrations are at a minimum in the summer (Mauritsen et al., 2011; Heintzenberg et al., 2015) with typical ~~values~~ accumulation mode concentrations less than 100 cm^{-3} and sometimes less than 1 cm^{-3}. Such low concentrations may be insufficient to maintain clouds (Mauritsen et al., 2011; Stevens et al., 2018; Sterzinger et al., 2022). ~~However,~~

One idea regarding how these low-level clouds can be maintained in the face of such low accumulation mode concentrations is that Aitken mode particles become important for cloud droplet activation (Bulatovic et al., 2021). This idea is supported by observational evidence suggesting that Aitken particles contribute to CCN populations in the Arctic (Willis et al., 2016; Koike et al., 2019; I and in many cases even dominate the CCN population (Karlsson et al., 2021, 2022; Siegel et al., 2022). The importance of the Aitken mode for cloud droplets has also been suggested in Southern Ocean low-level clouds (McCoy et al., 2021). The observations are supported by large eddy simulations and show that supersaturation in these low-level high latitude clouds can be large enough to activate Aitken particles (Bulatovic et al., 2021; Wyant et al., 2022). However, Bulatovic et al. (2021) found that when Aitken mode concentrations are low, the accumulation mode concentrations are most likely also low. That is, when accumulation mode concentrations are low, there may not necessarily be enough Aitken particles to sustain the low-level clouds either.

It has also been shown that measurements taken at the surface may not be representative of the rest of the lower atmosphere. Aerosol concentrations have been observed to be higher in the free troposphere (FT) than in the boundary layer (BL) (Lonardi et al., 2022; Creamean et al., 2021; Wylie and Hudson, 2002; Hegg et al., 1995; Igel et al., 2017). More specifically, using tethered balloon data from Oliktok Pt, Alaska spanning late spring 2017 through early fall 2018, Creamean et al. (2021) found that above cloud aerosol concentrations were higher than those below cloud in 38% of profiles analyzed. Lonardi et al. (2022) and Igel et al. (2017), using summertime data from the high Arctic, similarly found higher concentrations of tropospheric aerosol concentrations when compared to the surface, but these studies presented data from a limited number of days (four days in Igel et al. (2017) and three days in Lonardi et al. (2022), both over a week and a half timeframe).

It has been found that entrainment of aerosol particles above the inversion can be an important source of aerosol for the Arctic boundary layer (Igel et al., 2017; Price et al., 2023). As such, while the activation of Aitken particles may be one way to maintain low-level clouds when accumulation mode particle concentrations are ultra-low, the continuous entrainment of accumulation mode particles at cloud top may be another way.

In this study, we first analyze the entire tethered balloon dataset from MOSAiC (Pilz et al., 2022a) for further evidence that enhanced aerosol concentrations frequently exist above the boundary layer top and to determine whether there are any consistent changes in the size distribution across the boundary layer top. We then use idealized modeling to investigate the sensitivity of Arctic mixed-phase boundary layer clouds to aerosol concentrations in the free troposphere - specifically aerosol that can act as cloud condensation nuclei. We present a suite of simulations, each with different tropospheric aerosol

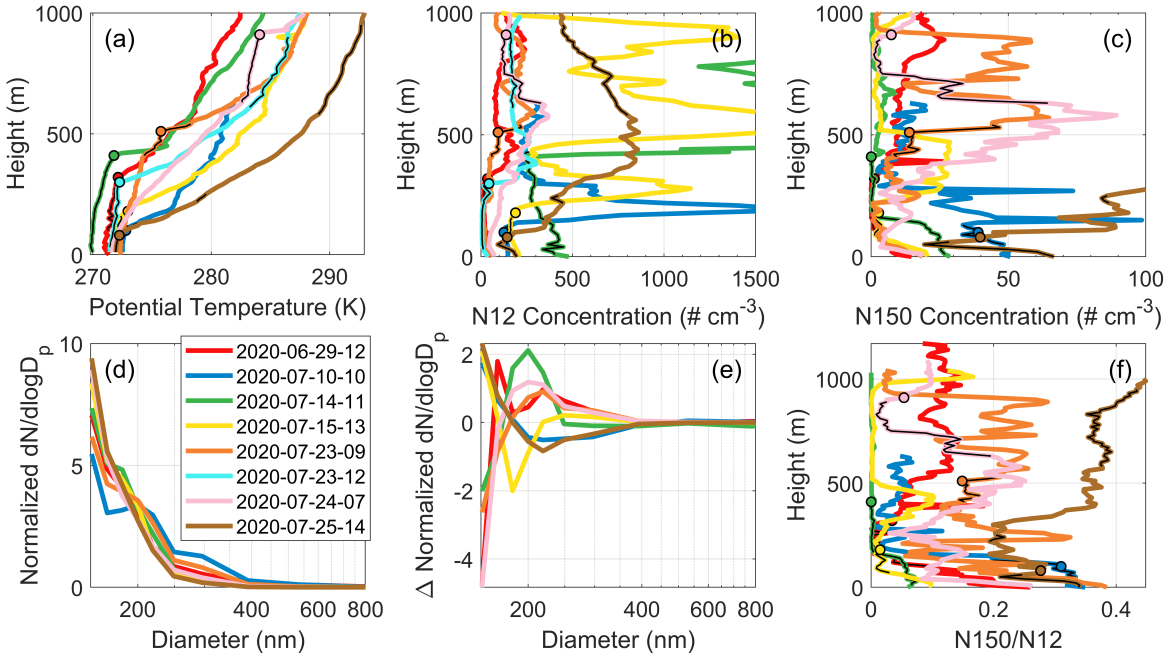

Figure 1. Profiles of (a) potential temperature, (b) concentration of particles with diameter >12 nm (N12), (c) concentration of particles with diameter >150 nm (N150), and (f) the ratio of N150 to N12 for select tethered balloon flights during the MOSAiC campaign. Black outlined circles represent the top of the mixed layer for each profile. Thin black lines indicate the most likely location of a cloud layer. (d) Normalized distributions averaged over 100m above the mixed layer top and (e) the normalized size distribution averaged over 100 m above the mixed layer top minus the normalized size distribution averaged 100 m below the mixed layer top.

concentrations and examine the effect of these varied concentrations on aerosol, cloud, and boundary layer properties. Finally, we briefly examine the sensitivity of our results to thermodynamic conditions.

2 Tethered Balloon Observations

Here we extend the analysis presented by Lonardi et al. (2022) to include all BELUGA (Balloon-bornE moduLar Utility for profilinG the lower Atmosphere) tethered balloon profiles from the high Arctic collected during MOSAiC (Shupe et al., 2022) with a well-defined temperature inversion to mark the transition to the free troposphere that is at least 100m below the profile top ~~(?). Figure 1~~ (Pilz et al., 2022b). We identified eight balloon flights that meet these criteria, only two of which were shown in Lonardi et al. (2022) (23 July 2020 beginning at 0901 UTC and 24 July 2020). These flights occur over about one month. Coincident measurements of cloud presence (Lonardi et al., 2022b) and radiation properties (Lonardi et al., 2022a) with the aerosol concentration measurements (Pilz et al., 2022a) are typically not available, but are instead frequently available an hour or two prior to the collection of the aerosol data. We use a combination of the cloud presence flags (available for only two

flights), the broadband fluxes, and the relative humidity to make a best guess at the extent of cloud layers for each aerosol data flight. Typically these layers seem consistent with the potential temperature profiles despite the measurements not be coincident in time (1a). Figure 1a-c shows vertical profiles of potential temperature and aerosol concentration for particle diameters >12 nm ~~from these days.~~ (N12) and >150 nm (N150) for all eight identified flights. Flight data has been binned and averaged over 10m height bins. The extent of the cloud layers is shown with overlaid thin black lines. Note that even though cloud layers are identified, the aerosol measurements may or may not have occurred in clear skies.

All aerosol profiles (Fig. 1b) have higher N12 concentrations above the inversion than at any level below the inversion with the exception of 24 July 2020. The N150 data is noisier; most profiles do show higher concentrations just above the inversion compared to below, but this could just be the result of aerosol scavenging by the cloud layer, such as is possibly evident on 29 June, 14 July, and/or 15 July. While the N150 data are more relevant for cloud droplet activation, there is growing evidence that Aitken mode particles contribute to droplet formation in environments with low accumulation mode concentration (Karlsson et al., 2021, 2022; Siegel et al., 2022). Therefore, both the N12 and N150 profiles are relevant for cloud layers in the Arctic. Some profiles show free-tropospheric N12 aerosol concentrations in the low 100s cm^{-3}, while others are seen to reach 1000 cm^{-3} or more. In all but one profile, the N150 concentrations are less than 100 cm^{-3} throughout the lowest 1km of the atmosphere. In all profiles, near-surface N12 aerosol concentrations were quite low, most below 200 cm^{-3} and some well below 100 cm^{-3}, despite the higher concentrations in the free troposphere.

~~Igel et al. (2017) found that entrainment of such elevated concentrations~~ Although the number of in situ observations of above-inversion aerosol concentrations in the high Arctic remains low, there is increasing evidence that the concentration of aerosol particles ~~above the inversion can be an important source of aerosol for the Arctic boundary layer. Shupe et al. (2013) found that the large aerosol particles needed to form and sustain Arctic stratocumulus were predominantly advected from lower latitudes. It may be that with too few aerosol in the boundary layer , entrainment of aerosol from the troposphere is necessary to sustain clouds for the duration observed in studies such as Shupe et al. (2011) and Morrison et al. (2012). Without sucha source of aerosol , clouds may exist in a tenuous regime and further dissipate (Sterzinger et al., 2022; Mauritsen et al., 2011).~~ is higher above immediately above the inversion than at the surface more often than not during the summer months.

~~(a) Potential temperature and (b) aerosol concentration (>12 nm) for select profiles during the MOSAiC campaign. Black dots represent the top of the boundary layer for each profile.~~

~~Many modeling studies of Arctic cloud-aerosol processes (e.g. Sterzinger et al., 2022; Stevens et al., 2018) rely on near-surface measurements of aerosol concentrations to initialize concentrations throughout the entire domain. Given 1)the decoupling from the surface so often seen in~~ We can also examine the size distribution of aerosol particles for particles with diameters >150 nm with the BELUGA data. The normalized size distributions averaged over the 100m above the mixed layer top show that the modal diameter in all cases is 150 nm or less (Fig. 1d). As such, from this data alone, it is difficult to determine a mean aerosol particle size. Nonetheless, we can take a difference in the normalized distributions averaged over 100 m above and below the mixed layer top to get a sense for whether there is a shift in the size distributions (Fig. 1e). Doing so reveals that there is no consistent trend among the flights; in some cases, the relative number of the ~~Arctic boundary layer and 2) a more polluted~~

troposphere being a potential source of aerosol for Arctic boundary layer clouds, it's likely that these surface measurements are not always representative of the aerosol concentrations influencing the cloud layer (Igel et al., 2017).

In this study, we use idealized modeling to investigate the sensitivity of Arctic mixed-phase boundary layer clouds to increased concentrations in tropospheric aerosol - specifically aerosol that can act as cloud condensation nuclei. We present a suite of simulations, each with different tropospheric aerosol concentrations and examine the effect of these varied concentrations on aerosol , cloud, and boundary layer propertiessmallest particles (sizes near 150 nm) increase and the relative number of larger particles decrease whereas in other cases the opposite is true. Likewise, there is no consistent trend in the ratio of N150 to N12 as a function of height (Fig. 1f). In the model simulations that follow, we will assume that there is no change in the mean size of the aerosol population across the boundary layer top.

3 MethodologyModel Simulations

3.1 Model and Simulation Setup

We used the Colorado State University Regional Atmospheric Modeling System (RAMS; Cotton et al., 2003) to run large eddy simulations , a scale at which RAMS has been used successfully in prior studies (e.g. Cotton et al., 1992; Jiang et al., 2001; Jiang and Feing and has proven to be insightful in studying aerosol-cloud interactions in Arctic clouds in similar LES setups (Bulatovic et al., 2021; Sterzing .

of Arctic low-level clouds. RAMS uses a double-moment bulk microphysics scheme (Walko et al., 1995; Meyers et al., 1997; Saleeby an (Meyers et al., 1997; Saleeby and Cotton, 2004) predicting hydrometeor mass and number concentrations for cloud, rain, ice, snow, aggregates, graupel, and hail. The scheme includes a prognostic aerosol treatment (Saleeby and van den Heever, 2013) which tracks prognoses the aerosol mass and number as well as accounting for removal by hydrometeor formation and regeneration by hydrometeor evaporationconcentrations. When aerosol particles activate to form droplets or ice crystals, the aerosol mass is tracked within the hydrometeor categories. Cloud droplets are activated from aerosol particles using Köhler theory by referencing lookup tables (Saleeby and Cotton, 2004) and hydrometeor diffusional growth is explicitly dependent on supersaturation. Dry and wet deposition of aerosols is included (Saleeby and van den Heever, 2013), but new particle formation is not parameterized in the RAMS aerosol scheme. Ice nucleation is parameterized following DeMott et al. (2010) as described in Saleeby and van den Heever (2013). Both CCN and INP are Aerosol particles are regenerated upon hydrometeor evaporation and the aerosol mass returned to the atmosphere upon complete evaporation of liquid drops and complete sublimation of ice particles, respectively. Secondary ice production is included via the Hallett-Mossop (rime splintering) processis proportional to the fraction of hydrometeor mass that was fully evaporated.

In order to investigate the aerosol impacts on the liquid phase alone, the model was modified to have separate categories for aerosol able to act as cloud condensation nuclei (CCN) and ice nucleating particles (INP). Salt was chosen as the aerosol category that would only serve as CCN, as it is totally soluble and cannot act as INP. Dust was chosen as the aerosol acting as INP; routines that allowed liquid nucleation onto dust were deactivated. While dust is known to act as CCN, the DeMott parameterization makes no distinction between immersion and deposition freezing - only the total number of particles, in or

out of droplets, is required. Therefore, we think that this separation approach is appropriate. In this study, we are concerned solely with the impacts of CCN on mixed-phase Arctic clouds - this separation of CCN and INP will allow for future study on the impact of INP alone. Furthermore, most of the simulations in this study are run at temperatures that are only slightly supercooled; ice is negligible in these simulations and will not be discussed.

~~In our configuration,~~ Longwave radiation is parameterized by BUGSRAD, a two-stream radiation model (Stephens et al., 2001) ~~.~~ that includes a dependency on the effective radius of cloud droplets and ice crystals. Despite ultra-low aerosol concentrations typically occurring during the summer, we neglect shortwave radiation to avoid the complications of a diurnal cycle and to avoid needing to tie our simulations to a specific day of the year. Subgrid-scale turbulence and diffusion is based on Deardorff (1980) - this scheme parameterizes eddy viscosity as a function of resolved turbulent kinetic energy (TKE). Surface fluxes were set to zero to provide an idealized framework in which cloud processes can be examined without influence from the surface~~, similar to conditions over an Arctic ice sheet during polar night with little surface heat and moisture fluxes. This removal~~ . The surface roughness length for momentum is set to 5×10^{-4}m. These surface assumptions are supported by observations of surface fluxes ~~also acts to simulate a boundary layer that is decoupled from the surface, which is often seen~~ in the Arctic ~~(Brooks et al., 2017)~~(Schröder et al., 2003).

The simulations in this study follow a similar setup to those in Sterzinger et al. (2022): a 6×6 km^2 periodic domain with 62.5 m horizontal and 6.25 m vertical grid spacing. Model top was set at ~~1250 m.~~ 1500 m. Simulations were run for a simulated 30 hours with a 1 second time step. The model was initialized with ~~the thermodynamic profile shown in Figure 2a. The cloud layer was added with an adiabatic profile of liquid water over a cloud layer 300 m thick that integrated to a liquid water path (LWP)~~ analytic thermodynamic profiles. A recent analysis of MOSAiC data by Jozef et al. (2023) showed that in the Arctic summer, boundary layers with very shallow mixed layers less than 125m deep are about as common as deeper, near-neutral layers. Both are frequently associated with low clouds and both are most frequently capped by inversions of 5K per 100m or stronger. Our base setup, in terms of inversion strength and boundary layer stability, is consistent with this latter cloud-bearing regime. Analytic profiles rather than case-based profiles are chosen so as to be able to easily modify them in thermodynamic sensitivity tests which will be described below. These profiles (BASE) are given by:

$$\theta(z) = \begin{cases} \theta_0, & z \leq 700 \text{ m} \\ \theta_0 + a(z-700), & 700 \text{ m} < z \leq 800 \text{ m} \\ \theta_0 + 100a + 0.005(z-800), & z > 800 \text{ m} \end{cases} \quad (1)$$

$$w(z) = \begin{cases} w_0, & z \leq 700\text{m} \\ w_0 + \frac{0.75 w_s(800) - w_0}{100}(z-700), & 700\text{m} < z \leq 800\text{m} \\ \frac{0.75}{2} w_s(z)(e^{-\frac{z-800}{200}} + 1), & z > 800\text{m} \end{cases} \quad (2)$$

where z is the height above the surface in meters, θ is potential temperature, w is the water vapor mixing ratio, and w_s is the saturated mixing ratio. For the BASE simulation, $\theta_0 = 273.15$ K, $a = 0.06$ K m^{-1}, and w_0 is the mixing ratio that gives 100% relative humidity at cloud base. We use a cloud that is initially 150m thick, and as such, $w_0 = 2.7$ g kg^{-1}.

We do not explicitly initialize cloud water. Instead, the potential temperature and water vapor profiles produce relative humidity well in excess of 100% in the cloud layer. Excess water vapor is converted to cloud water by the model and the associated latent heat of condensation is added to the temperature profile. Since it is these conditions - those after the model has modified the profiles that we provide in the input files - that are of ~~63 g m^{-2}; this is similar to the median LWP of 67 g m^{-2} measured over the ASCOS campaign (Mauritsen et al., 2011).~~ most interest for understanding the model setup, we show profiles of potential temperature, water vapor, and cloud mixing ratio shortly after model initialization in Figure 2a-b in blue. Winds are calm and nudging of the profiles to the initial condition is not performed. Large-scale subsidence prescribed by a fixed divergence rate of ~~5.0~~6.0$\times 10^{-6}$ s^{-1}. This value was chosen to prevent the boundary layer top from rising too rapidly.

~~Simulations were run for a simulated 28 hours with a 1 second integration period. The simulation was initialized to occur on October 1st at 85°N, a location which is in near-total twilight at this time of year. October also corresponds to the time of year when the aerosol concentrations in the Arctic BL are lowest (e.g. Boyer et al., 2023), and as such when entrainment of aerosol from the FT would likely be the most impactful. The model was run for two hours with a quasi-constant aerosol concentration to allow the cloud to spin-up. The prognostic aerosol scheme was turned on after this point, and an additional two hours are given to adjust - analysis in this study is for a 24-hour period beginning at the 4 hour mark.~~

To test the sensitivity to tropospheric CCN concentrations, a suite of simulations were run across a range of tropospheric salt concentrations. A baseline simulation with a salt aerosol particle concentration of 20 mg^{-1} at all levels was run. ~~Sensitvitity~~ Sensitivity tests were run in which salt concentrations in the FT were set by multiples of 200 mg^{-1} until a concentration of 1000 mg^{-1} (Fig. 2~~b~~c). These concentrations were chosen to be representative of the range of observed aerosol concentrations in the Arctic troposphere, with 1000 mg^{-1} being a high, but not unrealistically high, value (~~Figure 1).~~ Fig. 1b). The concentration in the inversion layer linearly increases with height from 20 mg^{-1} to the FT concentration. In all simulations, the aerosol particles were lognormally distributed with a modal diameter of 200 nm and a logarithmic standard deviation of 1.5. These parameters were kept constant with height given that we found no consistent trends in the change in size across the mixed layer top (Fig. 1e-f). For all of these CCN sensitivity simulations, dust concentrations were set at 20 mg^{-1} in both the FT and BL.

Since salt concentrations are the only aerosol species being modified in this study, from this point forward any mention of 'aerosol' is in reference to salt/CCN particles alone unless specified otherwise.

Finally, to test the sensitivity of our conclusions to the initial thermodynamic profile, we run an additional set of simulations with salt concentrations of 400 and 1000 mg^{-1} in the FT. These include tests in which the temperature inversion strength is halved, that is, $a = 0.03$ K m^{-1} in Eq. 1 (MODINV, consistent with common "moderate" inversions found in Jozef et al. 2023), the surface temperature is decreased by 10K (COOLER, $\theta_0 = 263$K in Eq. 1), and a stable layer is introduced below the cloud layer (STABLE). The modified equations for the initial conditions in STABLE are given by:

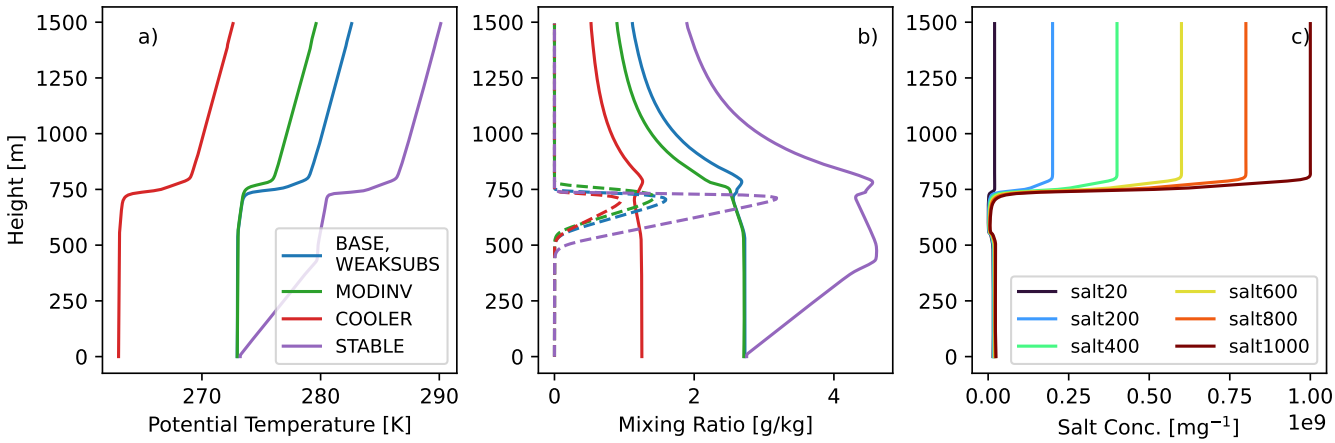

Figure 2. Profiles of (a) ~~Profile of~~ potential temperature~~(θ, blue line~~(b) water vapor mixing ratio (solid lines) and ~~relative humidity~~ cloud water mixing ratio (~~RH~~dashed lines; multiplied by 10 for clarity), ~~green line~~and (c) ~~used to initialize simulations~~salt aerosol profiles taken 30 minutes after simulation initialization. ~~Grey indicates the levels initialized as cloudy by adding an adiabatic liquid water profile.~~ Panels (a) and (b) ~~Salt aerosol~~ show profiles ~~used to initialize each of~~ for the ~~simulations~~base and thermodynamic sensitivity tests and panel (c) shows profiles for the salt experiments in the base setup.

4 ~~Results and Discussion~~

3.1 ~~Simulation Overview~~

$$\theta(z) = \begin{cases} \theta_0 + 0.015z, & z \leq 500 \text{ m} \\ \theta_0 + 7.5, & 500 \text{ m} < z \leq 700 \text{ m} \\ \theta_0 + 7.5 + a(z - 700), & 700 \text{ m} < z \leq 800 \text{ m} \\ \theta_0 + 7.5 + 100a + 0.005(z - 800), & z > 800 \text{ m} \end{cases} \tag{3}$$

$$w(z) = \begin{cases} w_0 - 4 \times 10^{-6}(700 - z), & z \leq 500 \text{ m} \\ w_0, & 500 \text{ m} < z \leq 700 \text{ m} \\ w_0 + \frac{0.75 w_s(800) - w_0}{100}(z - 700), & 700 \text{ m} < z \leq 800 \text{ m} \\ \frac{0.75}{2} w_s(z)(e^{-\frac{z-800}{200}} + 1), & z > 800 \text{ m} \end{cases} \tag{4}$$

In all cases, the initial cloud layer is 150 m thick. In STABLE, the mixing ratio profile gives a relative humidity that is nearly identical to that in BASE. We note that in STABLE, because the surface potential temperature is the same as in BASE, the cloud layer itself is warmer than in BASE. Finally, simulations are run which are identical to BASE except that the subsidence

rate is halved (WEAKSUBS). Thermodynamic profiles for all of these tests shortly after model initialization are shown in Figure 2a-b.

4 Model Simulation Results

4.1 Microphysical Response

~~The clouds produced by the six simulations are shown in Fig. 3. Liquid water mixing ratios (Fig. 3a) are relatively consistent for the higher aerosol concentration simulations, with cloud top mixing ratios of around 0.2 g kg^{-1}. While the cloud does display the typical mixed-phase stratocumulus setup of a layer of supercooled liquid above precipitating ice, ice production (Fig. 3b)was quite low and ice masses only reached 0.1 - 0.2 mg kg^{-1}. The beginning of the analysis period shows a large amount of ice (>0.2 mg kg^{-1}), this is residual ice from the quasi-constant aerosol treatment during the spin-up period. After this point, ice production is sustained in salt600 and above, whereas salt20, salt200, and salt400 are unable to sustain substantial ice production.~~

~~Figure 4a shows the liquid water path (LWP)of all six simulations from 4-28 hours~~The clouds produced by the six simulations are shown in Fig. 3. Clouds appear to have quasi-steady cloud tops for the higher aerosol concentration simulations (by design), with cloud top mixing ratios of around 0.35 g kg^{-1}. There is a strong sensitivity to FT aerosol concentration, with simulations initialized with FT salt concentrations of ~~20~~ 20-400 mg^{-1} ~~and 200 mg^{-1}~~ dissipating or nearly dissipating within 10-20 hours, while the simulations initialized with concentrations of ~~400~~ 600 mg^{-1} or higher are able to persist for the entire simulation period - though ~~salt400 may be~~ salt600 is headed toward dissipation. ~~The LWP response appears to be non-linear, with differences between simulations lessening with each subsequent increase in tropospheric aerosol concentration. Salt800~~ Salt600, salt800 and salt1000 are similar for the first ~~10-15 hours ,~~ 10 hours or so but start to diverge after this time. All simulations produce some rain water (Fig. 4~~e~~b). For ~~salt400~~ salt800 and above, the rain water is ~~about 10% of less of~~ a small fraction of the total liquid water. As seen by a lack of liquid water in the domain mean ~~between the surface and 400m~~ near the surface (Fig. 3~~a~~), very little rain water actually reaches the surface. Surface precipitation rates are at most 1.2 mm per day, which is essentially negligible and not large enough to be observed. Rather, the vast majority of the little rain that ~~there is is~~ exists is quickly evaporated below cloud base.

~~Figure 4b shows the evolution of ice water path (IWP) for each simulation. These values are on the extreme low end of typical IWP, a range of 0.1-120 g m^{-2} was reported in Shupe et al. (2008) as the 5th-95th percentile, respectively. Ice number concentrations (not shown) are also low, consistently between 0.1-0.2 L^{-1} after stabilizing from the spin-up period, again about an order of magnitude fewer than typical values around 1 L^{-1}, though as the dust concentrations are themselves low (to represent an aerosol-limited environment), this is perhaps not especially concerning. Underproduction of ice is not a new problem - representation of proper ice and liquid quantities together in models has been a persistent issue (Klein et al., 2009; Stevens et al., 2~~

~~Although dust concentrations were not changed between simulations, there was a response in ice to changes in cloud liquid. As expected, the ice phase of the cloud is dependent on the existence of the liquid phase. Salt20 and salt200, which have~~

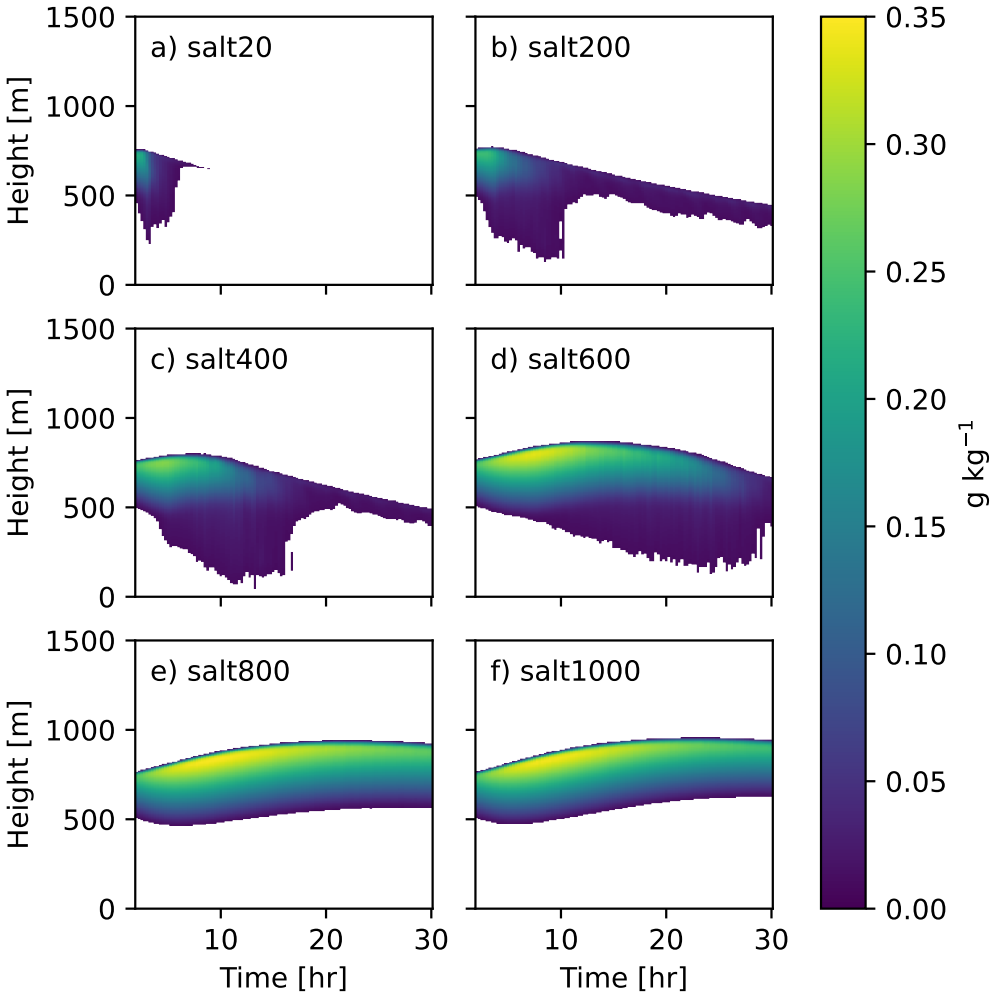

Figure 3. Time-height contours of ~~(a)~~ total liquid water ~~and (b) ice mass mixing ratio~~for all six base simulations. ~~Regions where cloud~~ The minimum liquid water ~~mass~~ mixing ratio shown is ~~greater than~~ 0.01 g kg^{-1} ~~are considered cloudy, regions where ice water (sum of all ice categories) mass is greater than 0.1 mg~~. The black line denotes a 0.01 g kg^{-1} ~~are considered icy. High ice concentrations at the beginning~~ contour of ~~the analysis period are leftover from high ice generation during the spin-up period~~cloud water alone.

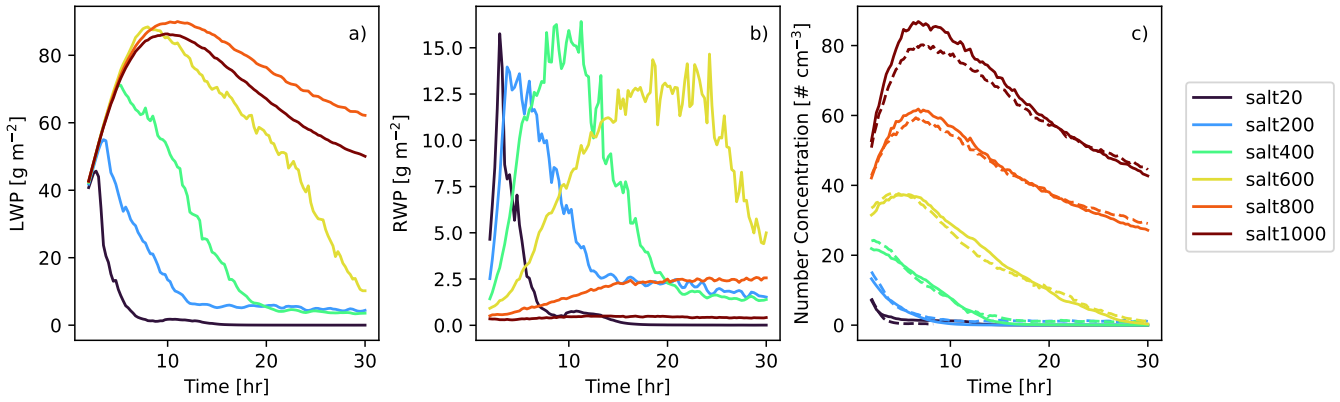

Figure 4. (a) Liquid water path, (b) ~~ice~~ rain water path for each base simulation, and (c) ~~rain water path for each simulation~~surface aerosol concentrations (solid) in the lowest model level and mean cloud droplet number concentrations (dashed) within the cloud layer. The ~~spin-up period (~~first ~~4~~ two hours ~~) is not shown~~are omitted.

~~rapidly depleting liquid with time (Figs. 3a, 4a) are unable to sustain ice without the liquid water whereas salt600, salt800, and salt1000 all maintain nearly constant IWP after hour 10. Since this study is to investigate the effect of aerosol that act as CCN alone, and such ice mass is very low compared to liquid, the rest of this study will be focused solely on liquid properties and processes.~~

4.2 ~~Surface Aerosol~~

~~The base simulation, salt20, was initialized with a uniform salt concentration of 20 mg^{-1} in both the BL and FT and dissipated in a manner similar to previously modeled cases of aerosol-limited dissipation (Sterzinger et al., 2022). Since the BL~~ Since the BL aerosol concentration is initialized to 20 mg^{-1} in all simulations, any changes in cloud liquid properties must come from tropospheric aerosol being entrained into the cloud layer.

~~Evolution of surface aerosol concentrations (solid) in the lowest model level and mean cloud droplet number concentrations (dashed) within the cloud layer.~~

~~Figure ??~~ As such, we now look to how the boundary layer aerosol concentrations and droplet concentrations respond to the FT aerosol concentration. Figure 4c shows the domain-mean salt number concentration directly above the surface in the lowest model level (solid lines) as well as the average cloud droplet concentration (dashed lines). ~~Aerosol concentrations decrease in time for the period shown, most likely due to surface deposition and reduction in particle concentrations due to weak collision-coalescence.~~ As is expected, the simulations initialized with higher aerosol concentrations in the free troposphere also have higher concentrations in the boundary layer due to transport of aerosol into the BL via either activation of FT aerosol at cloud top and subsequent hydrometeor evaporation in the boundary layer or by direct transport from the FT without being activated Igel et al. (2017). In all cases the BL aerosol concentration (less than ~~50 mg^{-1}~~ about 80 cm^{-3} for all simulations) remains ~~much~~ an order of magnitude lower than what was initialized in the FT. ~~There is an approximately linear increase in~~

surface aerosol number concentration similar to the linear increase in initialized FT aerosol shown in Figure 2b. Concentrations rapidly increase at the start of the simulations due to aerosol entrainment in salt600-salt1000. Eventually, aerosol concentrations decrease in time for all simulations, most likely due to dry and wet deposition and reduction in particle concentrations due to weak collision-coalescence. In salt20, without a large source of particles in the FT, surface concentrations are rapidly depleted within only a few hours after the simulations start. We note though that the rate of aerosol depletion in our simulations is likely unrealistically fast since our simulations lack sources of particles from the surface or from new particle formation.

These low surface aerosol concentrations show the dependence of a sustained cloud on the above-cloud aerosol. In all simulationsexcept salt 20, the average droplet concentration is higher than the surface aerosol concentration as a result of the entrainment of higher aerosol concentrations at cloud top. Furthermore, we note that a simulation initialized with 20 mg^{-1} of salt in the BL and FT(i.e. salt20) was unable to sustain itself, yet during most of the analysis period salt400 and salt600 - simulations with clouds that persist for the analysis period - have BL concentrations below 20 mg^{-1}. An observer with surface data alone could infer that this concentration is what is needed to sustain a cloud, when in reality the cloud is dependent on sustained FT aerosol entrainment to survive.

4.2 Precipitation suppression

The LWP response described in the section above is due largely to a precipitation suppression effect. An increase in aerosol concentrations divides the available water vapor across a larger number of nucleated droplets, decreasing their average size. These smaller, but more numerous, aerosol are less efficient at colliding, coalescing, and growing large enough to fall out as drizzle or rain droplets (Albrecht, 1989). This processes has been observed to occur in warm-phase marine stratocumulus clouds over lower latitudes (e.g. Wood, 2005b), as well as in Arctic mixed-phase clouds (e.g. Peng et al., 2002) - though it's expected that some interactions between different cloud droplet sizes and ice deposition processes make such a process more complex than in liquid-only clouds.

Our The mean droplet concentration is very closely linked to the surface aerosol concentrations (Fig. 4c). As such, our simulations show an increase in droplet number concentration (N_d) and a decrease in mean droplet radius (r_d) with an increase in FT aerosol concentrations. Figure 5a shows profiles of N_d at various times throughout the simulation period, with profiles normalized to cloud top height and cloud bottom. There is an approximate linear increase in the profiles of N_d correlating to the linear increases in tropospheric aerosol droplet concentration with the linearly increasing tropospheric aerosol concentrations. All profiles show a sharp small increase in N_d at cloud top which becomes less prominent with time, consistent with the nucleation of a relatively high number of entrained aerosol particles . Outside of this layer of enhanced N_d, cloud droplet concentrations are relatively constant throughout the cloud, as previously seen in marine stratocumulus (Wood, 2005a). The mass mean cloud at cloud top. The mean cloud droplet radius (Fig. 5b) decreases with increasing aerosol concentrations. This effect is less pronounced in the simulations with the highest concentrations, as the mean radius scales with $N_d^{-1/3}$ assuming an equal amount of liquid mass being divided between an increasing N_d.

In each simulation, cloud droplet number concentrations are decreasing and mean radii are increasing in time. This is indicative of either a decrease in the availability of CCN in the boundary layer and/or a decrease in the amount of aerosol being

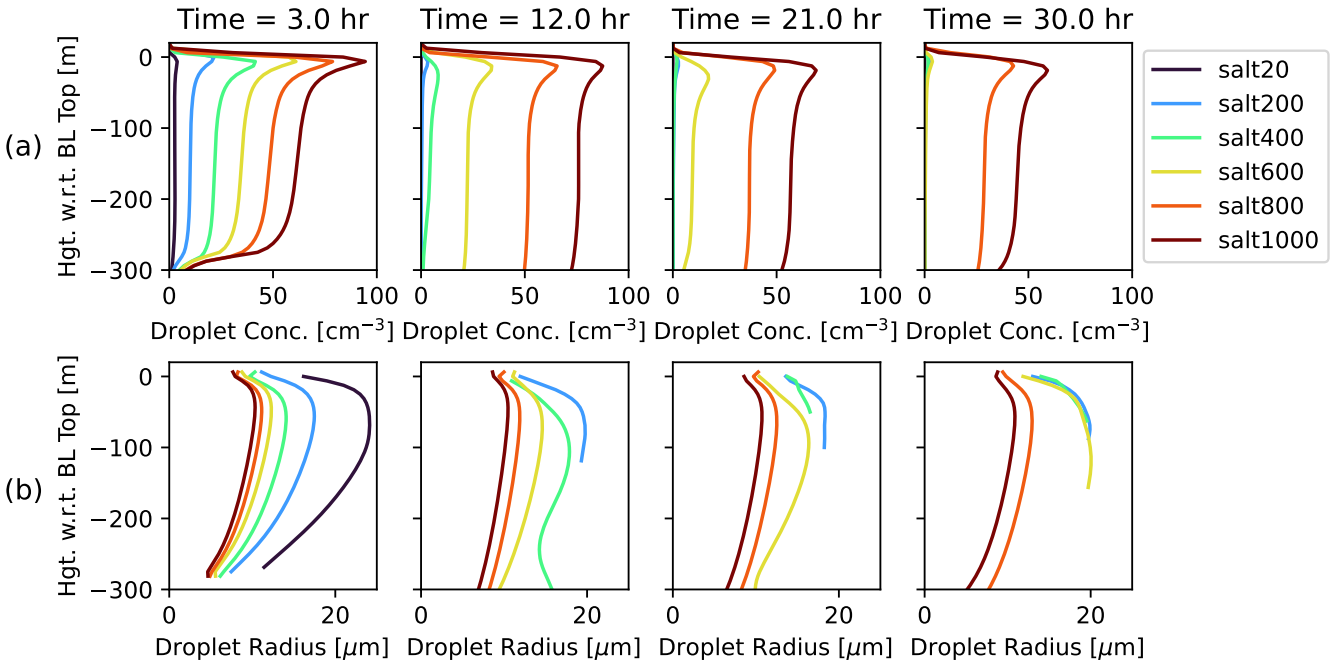

Figure 5. Evolution of (a) mean cloud droplet number concentration and (b) ~~mass mean~~ mass-mean cloud droplet radius profiles for all simulations every ~~8~~ 9 hours. The y-axes display heights ~~normalized~~ with respect to ~~cloud base and cloud~~ the boundary layer top.

~~entrained into the cloud (this can be seen by the decreasing surface salt concentrations in Fig. ??) andthus a fewer number of cloud droplets being nucleated. This effect is most pronounced in the lower concentration simulations, indicating that there are not enough~~ aerosol being entrained ~~to continue nucleating droplets. Salt200 persists as a very thin cloud, less than 40 m thick and wih LWP < 5 g m^{-2} (Figure 4a), with a very small number of relatively large droplets (< 1 cm^{-3} in number and 10-20 m in radius; Fig. 5).~~ into the cloud.

The result of the combined increase in cloud droplet number and decrease in radius is a reduction in collision coalescence efficiency. Figure 4c shows the rain water path (RWP) evolution for each simulation. There is clearly sensitivity to the tropospheric aerosol concentration with salt20 ~~and salt200~~ raining the most at the beginning of the simulation before dissipating~~, and salt400 and above producing rain throughout.~~ . The peak rain rate is delayed as the FT aerosol increases and salt1000 produces almost no rain at all. Such precipitation suppression has been commonly described in response to increasing aerosol concentrations in both warm- and mixed-phase stratocumulus clouds (e.g. Albrecht, 1989; Wood, 2005b; Peng et al., 2002). As noted above, although rain is being produced, very little rain actually reaches the surface. ~~The surface precipitation rates ...~~

~~This precipitation suppression process is the primary factor in the spread in LWP seen in Figure 4a. With aerosol concentrations too low, cloud droplets become larger and can completely rain out acloud, such as seen in salt20 and to a lesser extent in salt200. This process is less effective at higher concentrations, as the effects on mean droplet size decreases with increasing number. However, it is not the only process impacting the LWP. Sustained rain production, which is present even in salt1000, does not~~

~~imply dissipation so long as the rate of rain production is balanced by the production of new cloud water~~While salt20 simulates an essentially complete removal of aerosol and cloud water, salt200 and salt400 do not simulate complete dissipation of the clouds. Rather, salt200 and salt400 simulate persistent, very thin clouds, less than 40 m thick and wih LWP < 5 g m^{-2} (Fig. 4a), with a very small number of relatively large droplets (< 1 cm^{-3} in number and 10-20 μm in radius; Fig. 5). Some of this water resides in the rain category, but we note that this rain water is produced when the droplets grow by condensation to exceed the maximum allowed mean cloud droplet diameter of 50 μm (not shown). In this situation, some cloud water is transferred to the rain category. Collision-coalescence is minimal. In this state, there are no longer strong sinks of aerosol number concentration since any particle that is activated can be returned to the atmosphere upon drop evaporation. These thin clouds are still weakly turbulent. We do not know if such a state - one with very low LWP coincident with very low aerosol particle concentrations - commonly exists in the Arctic atmosphere. Certainly liquid-bearing clouds with LWP less than 25 g m^{-2} are frequently occurring (Silber et al., 2020; Sedlar, 2014). Alternatively, because the aerosol concentrations that are simulated are exceptionally low given our lack of particle sources in the model, the simulated clouds may not be representative of the Arctic atmosphere.

4.2 ~~Radiation and buoyancy impacts~~Thermodynamic Response

~~Radiative heating rate profiles every 8 hours of simulation time in the top 20% of the cloud layer. The heights are normalized to cloud top and bottom.~~

The precipitation suppression process is the primary factor in the spread in LWP seen in Figure 4a. However, it is not the only process impacting the LWP. As is expected, a change in a cloud's ~~amount of liquid water~~ liquid water path also affects its emissivity. Figure 6a shows a time series of the ~~radiative flux divergence~~ net longwave radiative flux difference across the cloud layer. This ~~is calculated as the difference in net flux (longwave and shortwave) between cloud top and cloud bottom. The flux divergence is dominated by longwave radiation; as these simulations were initialized at 85°N in early October, shortwave radiation is nonexistent most of the day and negligible for the 3-4 hours when the sun does peek above the horizon~~difference is equivalent to the vertically integrated longwave radiative cooling occurring in the cloud layer. There is a large spread in the flux ~~divergence~~difference, with around ~~50~~ 80 W m^{-2} separating salt600 and above from salt20 and salt200 ~~near the end of the simulation.~~ around hour 20. This radiative sensitivity to aerosol concentration is triggered first by the precipitation suppression effect described above. The less numerous, larger droplets created with fewer aerosol lead to the development of thin clouds with less liquid water, which do not behave as a blackbody but rather as a graybody. This radiative behavior of thin water clouds is consistent with previous work (Morrison et al., 2008; Shupe and Intrieri, 2004; Mauritsen et al., 2011; Garrett and Zhao, 2006). While generally longwave impacts of the aerosol indirect effects are seen as minimal (especially in thicker stratocumulus clouds in lower latitude), Morrison et al. (2008) found through modeling that changing aerosol concentrations had a longwave effect in thin clouds with LWP < 50 g m^{-2}. Shupe and Intrieri (2004) have a lower threshold of 30 g m^{-2} for this effect. Our results are consistent with these previous studies. Salt400, with its LWP of 50 g m^{-2} or less throughout most of the simulation, has an integrated radiative cooling that differs substantially from those for salt600 and above.

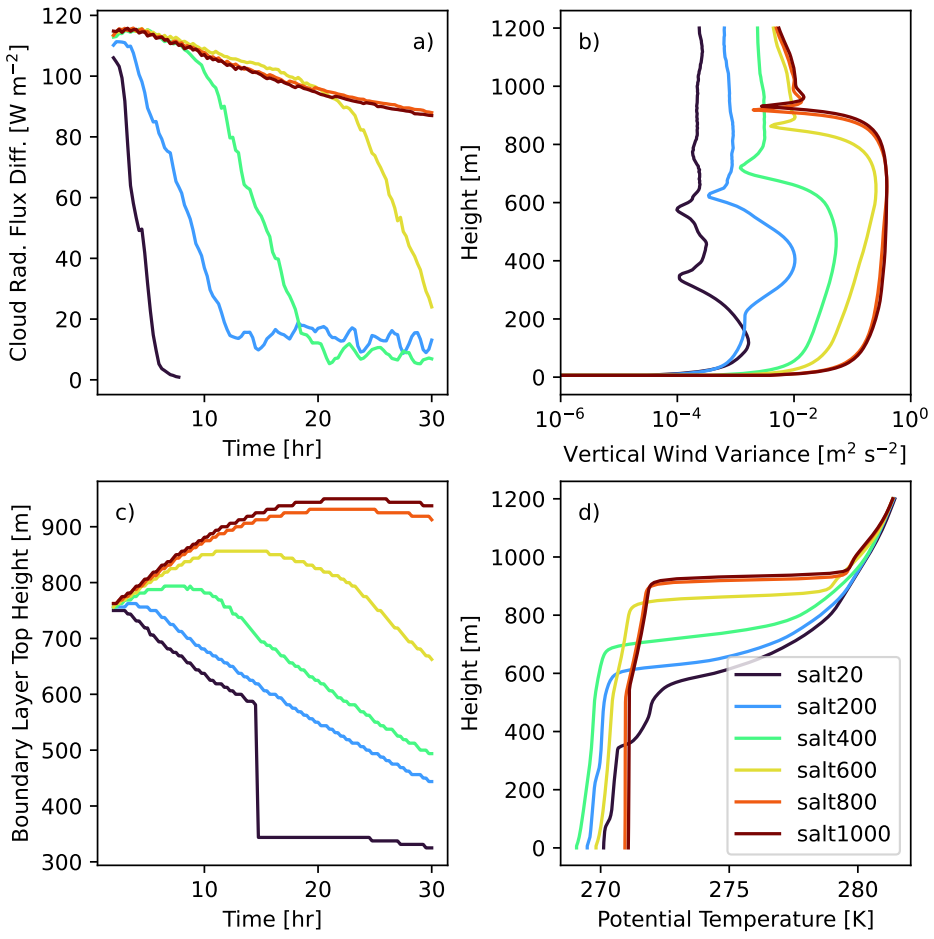

Figure 6. Time series of (a) radiative flux ~~divergence~~ difference across the cloud layer ~~,~~ and (c) boundary layer top height. Vertical profiles of (b) vertical wind variance (σ_w^2) ~~,~~ and (~~c) boundary layer top height. (~~d) ~~Profiles of~~ boundary layer potential temperature (θ) at the ~~end of the simulations.~~ hour 15.

This longwave sensitivity is important since, in the absence of surface fluxes, the cloud must be maintained from the top-down (cooling at cloud top drives an overturning buoyancy circulation) versus the from bottom-up (surface heat fluxes and BL instability drive vertical motions). As such, the dynamics of the cloud are sensitive to changes in radiative cooling rates within the cloud layer. ~~Figure ?? shows the radiative heating rate profiles every eight hours for the top 20% of the cloud. The higher LWPsimulations salt800~~ The much reduced cooling rates in the salt200 and ~~salt1000 show similar radiative heating rates throughout the simulation, but the lower aerosol concentration/LWP simulations produce a range of cooling rates , inline with the fluxes seen in Fig. 6a. Simulations with a decreasing LWP for most of the analysis period (salt20 - salt600) also have a decreasing radiative cooling rate in time. Increased cooling at cloud top drives a stronger overturning buoyancy circulation, further sustaining the cloud.~~ salt400 clouds contribute to the reduced LWP. At the same time, the reduced cooling rates help to maintain these clouds in their low LWP state by helping to reduce rain formation.

The vertical wind variance, which is the vertical component of turbulence kinetic energy (TKE) $\sigma_w^2 = \overline{w'w'}$, thus also has a sensitivity to the tropospheric aerosol concentrations. Figure 6b shows the domain-average ~~time series~~ vertical profile of σ_w^2 midway through the simulations. Simulations with higher aerosol concentrations drive stronger average vertical motions. The effect of increasing aerosol concentrations on vertical motions is more apparent at lower aerosol concentrations, where the clouds are thinner and increasing cloud droplet concentration and LWP has a ~~more profound~~ stronger effect on the longwave emissivity of the cloud. As clouds start to approach ~~as~~ a blackbody in salt600 and above, the difference in σ_w^2 becomes smaller. ~~Peak σ_w^2 occurs slightly below cloud top (not shown); at this location the negatively-buoyant downdrafts from cooling near cloud-top are at their strongest and these downdrafts drive the boundary layer circulations.~~

~~These radiative and dynamic effects are not responsible for the initial LWP response to aerosol, but are instead created initially by the precipitation production suppression and act as a positive feedback. This leads to stronger vertical motions in simulations with higher tropospheric aerosol concentrations. These stronger vertical motions help drive additional cloud droplet condensation, increasing LWP and feeding back into the cycle.~~

~~While generally longwave impacts of the aerosol indirect effects are seen as minimal (especially in thicker stratocumulus clouds in lower latitude), Morrison et al. (2008) found through modeling that changing aerosol concentrations had a longwave effect in thin clouds with LWP $<$ 50 g m^{-2}. Shupe and Intrieri (2004) have a lower threshold of 30 g m^{-2} for this effect. Our results are consistent with these previous studies. Salt400, with its LWP of 30-50 g m^{-2} throughout most of the simulation, has a flux divergence that differs substantially from those for salt600 and above. Mauritsen et al. (2011) also found that for clouds with low CCN concentrations, a tenuous cloud regime exists where radiative forcings start to tend towards zero faster than expected from the aerosol-cloud-albedo and cloud-lifetime affects alone. Garrett and Zhao (2006) also found that thin Arctic cloud emissivity is sensitive to changes in aerosol concentrations, as cloud emissivity (ε) changes with droplet size and as such these clouds act as a graybodies ($\varepsilon < 1$) not blackbodies ($\varepsilon \approx 1$) at small drop sizes.~~

4.3 ~~Boundary layer thermodynamics~~

~~The combined effects of increasing FT aerosol concentrations changes~~

~~Profiles of aerosol concentrations near the boundary layer top. Heights are normalized with respect to the boundary layer~~

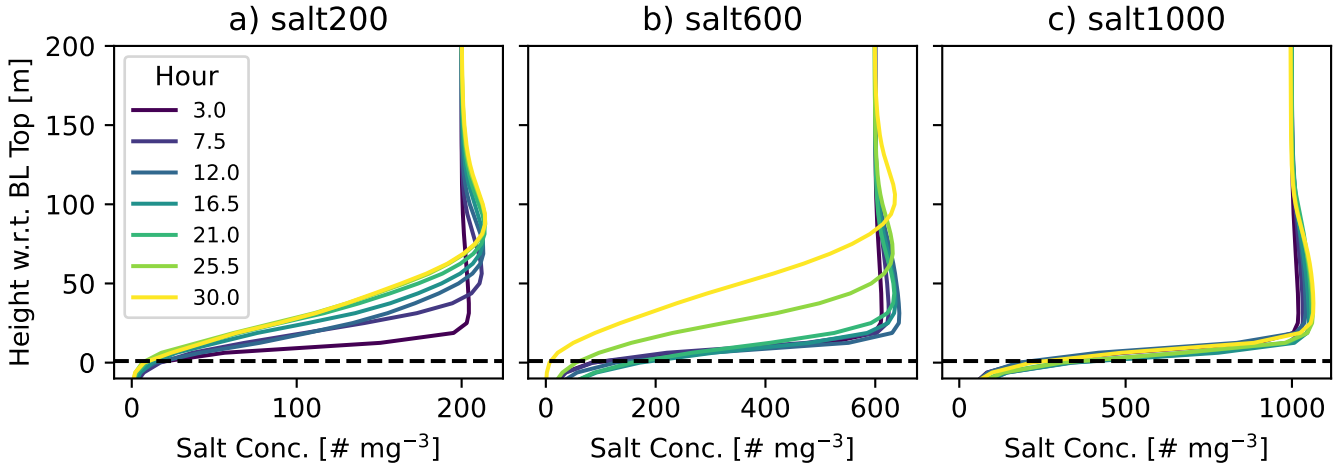

~~top.~~

Figure 7. Profiles of aerosol concentrations near the boundary layer top for salt200, salt600, and salt1000.

These changes to the turbulent mixing have consequences for the development of the boundary layer~~structure between simulations~~. Figure 6c shows the evolution of boundary layer top height (defined as the height ~~of the base of the temperature inversion~~with maximum curvature in the potential temperature profile) with time. In the higher aerosol simulations (salt800/salt1000), ~~this~~ the BL top is nearly constant in time after about hour 15 (by design). On the other extreme, salt20 ~~'s boundary layer top decreases nearly 300 meters in a 24 hour period, or around 0.35 cm/s. Accompanying the lowered BL tops are~~ develops a second inversion at the base of the dissipating cloud. Around hour 15, this inversion becomes stronger than the original inversion and our diagnosed BL top plummets from around 600 m to around 350 m. This double inversion structure in salt20 is seen explicitly in the potential temperature profile at hour 15 (Fig. 6d). Salt200 and salt400 do not have a total collapse of the cloudy mixed layer, but they do have rapidly descending BL tops accompanied by weakened temperature inversions (Fig. 6d). ~~These chagnes are unsurprising given the other results so far.~~ With surface fluxes disabled and without a cloud-driven circulation to drive entrainment, the large-scale subsidence will act to lower the height of the inversion and a lack of mixing will weaken the inversion. ~~Combined, these changes suggest that the boundary layer is collapsing in salt20.~~

~~The collapsing~~ Finally, the collapsing of the boundary layer has implications for aerosol entrainment and ultimately for the cloud's ability to maintain itself. Successful entrainment of tropospheric aerosol depends on a layer of enhanced aerosol concentration directly above the ~~cloud~~mixed layer. Figure 7 shows that in ~~salt20,~~ salt200 ~~, and (to a lesser extent)~~ and salt600 (and salt400, but not shown), a buffer develops between the aerosol in the FT and the top of the boundary layer. In these simulations, the boundary layer is collapsing ~~faster than the layer above can be replenished with aerosol by subsidence. In salt600~~ which leaves behind a layer of air with aerosol concentrations that are much lower than those is the rest of the free troposphere. In salt800 and above, the boundary layer top is ~~not lowering as quickly~~ maintained and is better able to stay in contact with the tropospheric aerosol reservoir. This is a likely factor in the faster decrease of BL aerosol concentrations in the ~~salt20 and salt400~~ salt20-salt400 simulations seen in Figure ~~??~~4c, and, more importantly, in the ability of clouds to sustain

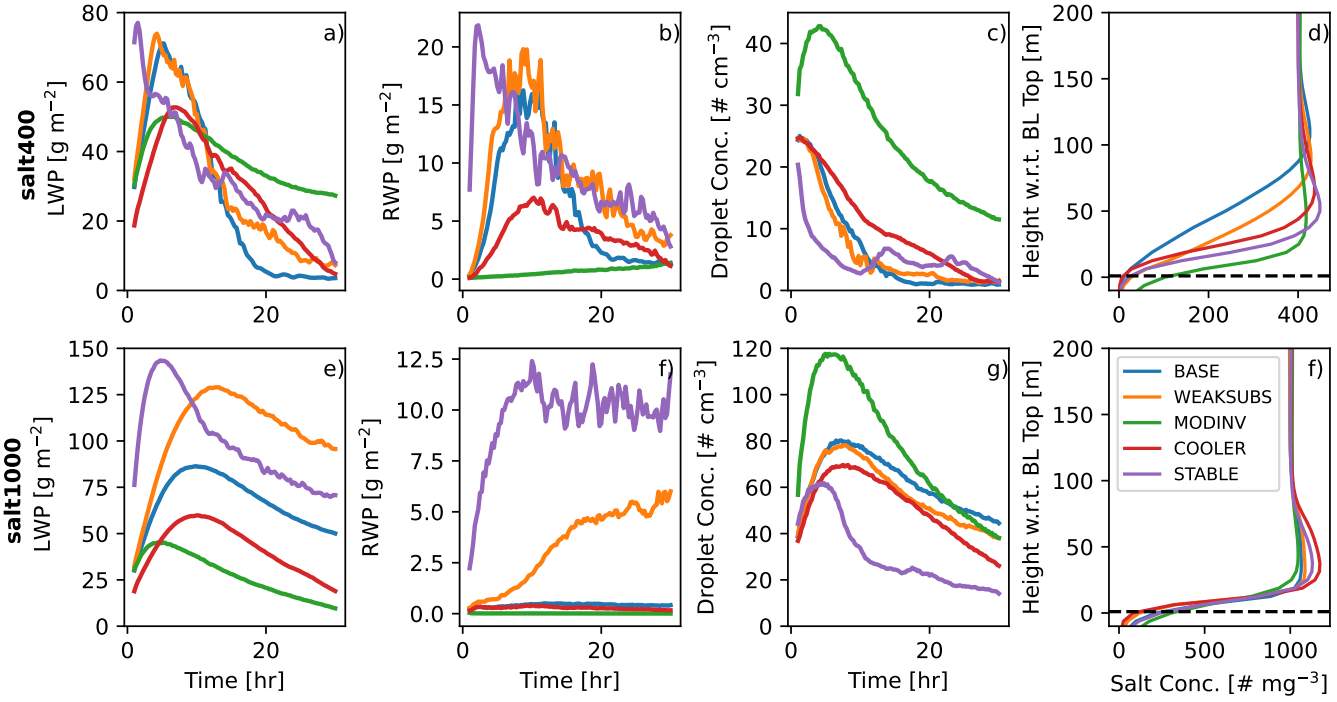

Figure 8. (a,e) Liquid water path time series, (b,f) rain water path time series, (c,g) mean cloud droplet number concentrations time series, and (d,f) salt concentration profiles at hour 30 for (a-d) salt400 sensitivity tests and (e-f) salt1000 sensitivity tests. The first two hours are omitted.

themselves in the face of very low boundary layer aerosol concentrations. As a result of the weakened turbulent mixing, the low FT salt simulations effectively cut themselves off from the reservoir of particles in the free troposphere.

4.3 Sensitivity Tests

Finally, we briefly look at the thermodynamic sensitivity tests that we ran. Salt400 reaches a nearly dissipated state in all but the test with the moderate inversion (MODINV), albeit the cloud water desiccation occurs more slowly than in the BASE set up (Fig. 8a). Longer cloud maintenance with a weaker inversion is unsurprising since the entrainment of aerosol particles should be faster. Indeed, we see that salt400-MODINV and salt1000-MODINV have the highest droplet concentrations (Fig. 8c,g) and that these are sufficient to suppress the rain water path (Fig. 8b,f). Salt400-MODINV is also the most successful in keeping the FT aerosol reservoir in contact with the boundary layer top, whereas the other salt400 tests show varying degrees of separation between the two (Fig. 8d). Salt1000 is much more sensitive to the initial thermodynamic conditions (Fig. 8e-g) than salt400. Most importantly though, in all tests the cloud is maintained throughout the simulation and good contact is kept between the boundary layer top and the aerosol reservoir (Fig. 8f). While certainly more time could be spent examining these tests, the primary point is that in the absence of other aerosol sources, a concentration of 400 cm^{-3} in the free troposphere may or may

not be sufficient to maintain a cloud, whereas a concentration of 1000 cm^{-3} appears more likely to be frequently sufficient, and that the processes that we describe in detail above that lead to the cloud desiccation appear to be occurring under these alternative thermodynamic conditions as well.

5 Conclusions

We present idealized LES simulations of an Arctic ~~mixed-phase~~ low-level cloud with various tropospheric ~~salt~~ aerosol concentrations (which ~~we refer to generally as 'aerosol', and which~~ serve only as CCN). A baseline simulation with low aerosol concentration (20 mg^{-1} of salt) in both the boundary layer and free troposphere simulated a cloud that was unable to sustain itself more than a few hours. Increasing tropospheric salt concentrations from 200 - 1000 mg^{-1} (in multiples of 200 mg^{-1}) ~~resulted in a positive LWPsensitivity~~increasing LWP. The lower aerosol concentration simulations ~~(200 mg^{-1} and below)~~ yielded clouds that either ~~did dissipate~~ dissipated within the simulation period or ~~were declining enough with respect to LWP, IWP, and radiative cooling rates that they were not likely to persist for much longer had the simulations been run for additional time~~persisted with very low LWP. The higher aerosol concentration simulations ~~(600 mg^{-1} and above)~~ produced clouds that ~~had more stable LWP and IWP. We find that tropospheric aerosol concentrations of more than 200 mg^{-1} were necessary for cloud persistence beyond about 24 hours. These concentrations are well within the range generally found in the lower free troposphere (Figure 1b and e.g. Lonardi et al., 2022; Jung et al., 2018). Given that the required concentrations are realistic, aerosol entrainment from the FT is likely important in the summertime high Arctic for maintaining low-level clouds.~~ maintained high LWP throughout all or most of the simulation period.

The cloud sensitivity to aerosol in the free troposphere is a result of entrainment and activation of aerosol particles from the troposphere into the cloud layer. This process causes three feedbacks that result in the change in liquid water content in the cloud:

- Increasing tropospheric aerosol concentrations leads to the commonly noted precipitation suppression effect. As more aerosol are entrained into the cloud layer and activated, the available liquid is divided among more droplets, causing an increase in cloud droplet number and a decrease in their size. This results in a less efficient collision-coalescence processes and thus less removal of water by rain.

- As a consequence of the rain suppression the higher liquid water content in the higher aerosol concentration simulations causes stronger cooling at cloud top. This cooling, which is primarily responsible for the circulations that maintain the cloud in the absence of surface forcing, drives stronger vertical motions in the clouds with higher droplet concentrations. ~~This processes is kickstarted by the change in liquid content caused by the precipitation suppression described above.~~

- Finally, due to these two processes, higher FT aerosol concentration simulations are better able to maintain contact between the FT aerosol reservoir and the boundary layer top in order to maintain the very aerosol entrainment that ~~causes~~ supports the precipitation suppression.

~~There is potential for tropospheric aerosol to be even a larger source of CCN due to the formation of a "cloud inside inversion" (CII) regime, which is a dominant regime over Arctic sea ice (Sedlar et al., 2012) but which was not simulated here. The presence of the cloud layer inside the inversion means that cloud droplets could nucleate directly within the free troposphere, without needing to be entrained through a temperature inversion first.~~

~~Our simulations produced surface aerosol concentrations that were representative of cloud droplet number concentrations. This is due to the coupled nature of the simulated boundary layer; had it been decoupled, the enhanced aerosol concentrations making their way into the boundary layer would likely not have been detectable at the surface. The observed surface concentrations were still much lower than those of the FT. In a real world situation similar to the one simulated, surface measurement of aerosol concentration - even alongside cloud droplet number concentration - would indicate that the cloud could persist with aerosol concentrations of 20-50~~ We find that tropospheric aerosol concentrations of more than 400 mg^{-1}~~. We find that simulations initialized with concentrations that low throughout the atmosphere do not produce stable clouds. Surface based measurements of this sort would not necessarily suggest the influence of FT aerosol on the cloud, despite it being necessary for stable cloud persistence. Even the most extreme simulation with initial FT aerosol concentrations of 1000 mg^{-1} (which has been observed to occur in the Arctic in Fig. 1b), producing the most stable cloud, yielded surface aerosol and cloud droplet number concentrations < 50 mg^{-1}.~~

~~We also note that the low ice mass and concentrations in this study simplified the discussion of processes impacted by increases in tropospheric aerosol. The liquid response would have likely been complicated in the presence of more ice, where processes such as the Wegener-Bergeron-Findeisen (WBF) process - in which cloud ice grows at the expense of evaporating liquid droplets - would likely have played a larger role in the cloud response.~~

~~The separation of aerosol in our methodology between those that can act as CCN and INP allows for a natural continuation~~ were necessary for cloud persistence beyond about 24 hours in most of the conditions that we tested. This concentration is only meant to be a very rough estimate which will of course depend on thermodynamic conditions and the size and hygroscopicity of the aerosol particles (which was rather high with our assumed salt particles). Nonetheless, it is encouraging that such concentrations are well within the range generally found in the lower free troposphere (Fig. 1b and e.g. Lonardi et al., 2022; Jung et al., 201 . Given that the required concentrations are realistic, continuous aerosol entrainment from the FT is likely important in the summertime high Arctic for maintaining low-level clouds. As discussed in the introduction, others have speculated that Aitken particles are important for explaining cloud maintenance under low aerosol conditions and found evidence of Aitken particle activation in these clouds (Bulatovic et al., 2021; Karlsson et al., 2021, 2022; Siegel et al., 2022). Here we present a second mechanism for maintaining a sufficient CCN supply that can work together with Aitken particle activation. A major limitation of this study ~~in which salt (CCN) concentrations and dust (INP) concentrations are varied in the free troposphere. In reality, of course, there is no such strict partitioning between CCN and INP, and the measurements of increased aerosol concentrations above the Arctic boundary layer naturally include both aerosol that can act as CCN and INP. Running similar modeling studies with more realistic aerosol treatment is critical to fully understanding the impact of these aerosol on Arctic cloud properties~~is that we did not include new particle formation in our simulations. Price et al. (2023) found that in the late summer in the Arctic boundary layer there is a transition from particle sources dominated by long-range transport and entrainment through

the boundary layer top to local new particle formation. As such, there is reason to believe that new particle formation may be important at this time of year. We also did not include Aitken particles in our simulations. Future work looking at the maintenance of clouds under low aerosol conditions should consider all of these processes.

Code and data availability. Tethered balloon data can be found on PANGAEA: meteorology data Pilz et al. (2022b), aerosol data Pilz et al. (2022a), broadband longwave radiation Lonardi et al. (2022a), and liquid water flags Lonardi et al. (2022b). Model source code and namelists used in this study can be found at https://doi.org/10.5281/zenodo.7991354 (Sterzinger et al., 2023). Horizontally-averaged processed model data used for analysis can be found at https://doi.org/10.5281/zenodo.7986917 (Sterzinger and Igel, 2023b). Code used to generate plots for this paper can be found at https://doi.org/10.5281/zenodo.7996595 (Sterzinger and Igel, 2023a).

Author contributions. LJS and ALI conceived the study. LJS and ALI conducted and analyzed the simulations. ALI analyzed the tethered balloon data. LJS wrote the original draft. LJS and ALI edited and reviewed the draft.

Competing interests. The authors declare no competing interests.

Acknowledgements. We thank two anonymous reviewers for their comments on the manuscript. This research was supported by the U.S. Department of Energy's Atmospheric System Research, an Office of Science Biological and Environmental Research program, under Grant No. DE-SC0019073-0.

References

Albrecht, B. A.: Aerosols, Cloud Microphysics, and Fractional Cloudiness, Science, 245, 1227–1230, https://doi.org/10.1126/science.245.4923.1227, 1989.

Boyer, M., Aliaga, D., Pernov, J. B., Angot, H., Quéléver, L. L. J., Dada, L., Heutte, B., Dall'Osto, M., Beddows, D. C. S., Brasseur, Z., Beck, I., Bucci, S., Duetsch, M., Stohl, A., Laurila, T., Asmi, E., Massling, A., Thomas, D. C., Nøjgaard, J. K., Chan, T., Sharma, S., Tunved, P., Krejci, R., Hansson, H. C., Bianchi, F., Lehtipalo, K., Wiedensohler, A., Weinhold, K., Kulmala, M., Petäjä, T., Sipilä, M., Schmale, J., and Jokinen, T.: A Full Year of Aerosol Size Distribution Data from the Central Arctic under an Extreme Positive Arctic Oscillation: Insights from the Multidisciplinary Drifting Observatory for the Study of Arctic Climate (MOSAiC) Expedition, Atmospheric Chemistry and Physics, 23, 389–415, https://doi.org/10.5194/acp-23-389-2023, 2023.

Brooks, I. M., Tjernström, M., Persson, P. O. G., Shupe, M. D., Atkinson, R. A., Canut, G., Birch, C. E., Mauritsen, T., Sedlar, J., and Brooks, B. J.: The Turbulent Structure of the Arctic Summer Boundary Layer During The Arctic Summer Cloud-Ocean Study, Journal of Geophysical Research: Atmospheres, 122, 9685–9704, https://doi.org/10.1002/2017JD027234, 2017.

Bulatovic, I., Igel, A. L., Leck, C., Heintzenberg, J., Riipinen, I., and Ekman, A. M. L.: The Importance of Aitken Mode Aerosol Particles for Cloud Sustenance in the Summertime High Arctic – a Simulation Study Supported by Observational Data, Atmospheric Chemistry and Physics, 21, 3871–3897, https://doi.org/10.5194/acp-21-3871-2021, 2021.

Cotton, W. R., Stevens, B., Feingold, G., and Walko, R. L.: Large Eddy Simulation of Marine Stratocumulus Cloud with Explicit Microphysics, in: Proceedings of a Workshop on Parameterization of the Cloud Topped Boundary Layer. ECMWF, Reading RG29AX, UK, vol. 236, 1992.

Cotton, W. R., Pielke Sr., R. A., Walko, R. L., Liston, G. E., Tremback, C. J., Jiang, H., McAnelly, R. L., Harrington, J. Y., Nicholls, M. E., Carrio, G. G., and McFadden, J. P.: RAMS 2001: Current Status and Future Directions, Meteorology and Atmospheric Physics, 82, 5–29, https://doi.org/10.1007/s00703-001-0584-9, 2003.

Creamean, J. M., de Boer, G., Telg, H., Mei, F., Dexheimer, D., Shupe, M. D., Solomon, A., and McComiskey, A.: Assessing the Vertical Structure of Arctic Aerosols Using Balloon-Borne Measurements, Atmospheric Chemistry and Physics, 21, 1737–1757, https://doi.org/10.5194/acp-21-1737-2021, 2021.

Deardorff, J. W.: Stratocumulus-Capped Mixed Layers Derived from a Three-Dimensional Model, Boundary-Layer Meteorol, 18, 495–527, https://doi.org/10.1007/BF00119502, 1980.

DeMott, P. J., Prenni, A. J., Liu, X., Kreidenweis, S. M., Petters, M. D., Twohy, C. H., Richardson, M. S., Eidhammer, T., and Rogers, D. C.: Predicting Global Atmospheric Ice Nuclei Distributions and Their Impacts on Climate, Proceedings of the National Academy of Sciences, 107, 11 217–11 222, https://doi.org/10.1073/pnas.0910818107, 2010.

Garrett, T. J. and Zhao, C.: Increased Arctic Cloud Longwave Emissivity Associated with Pollution from Mid-Latitudes, Nature, 440, 787–789, https://doi.org/10.1038/nature04636, 2006.

Hegg, D. A., Ferek, R. J., and Hobbs, P. V.: Cloud Condensation Nuclei over the Arctic Ocean in Early Spring, Journal of Applied Meteorology and Climatology, 34, 2076–2082, https://doi.org/10.1175/1520-0450(1995)034<2076:CCNOTA>2.0.CO;2, 1995.

Heintzenberg, J., Leck, C., and Tunved, P.: Potential Source Regions and Processes of Aerosol in the Summer Arctic, Atmospheric Chemistry and Physics, 15, 6487–6502, https://doi.org/10.5194/acp-15-6487-2015, 2015.

Igel, A. L., Ekman, A. M. L., Leck, C., Tjernström, M., Savre, J., and Sedlar, J.: The Free Troposphere as a Potential Source of Arctic Boundary Layer Aerosol Particles, Geophysical Research Letters, 44, 7053–7060, https://doi.org/10.1002/2017GL073808, 2017.

Intrieri, J. M., Fairall, C. W., Shupe, M. D., Persson, P. O. G., Andreas, E. L., Guest, P. S., and Moritz, R. E.: An Annual Cycle of Arctic Surface Cloud Forcing at SHEBA, Journal of Geophysical Research: Oceans, 107, SHE 13–1–SHE 13–14, https://doi.org/10.1029/2000JC000439, 2002.

Jiang, H. and Feingold, G.: Effect of Aerosol on Warm Convective Clouds: Aerosol-cloud-surface Flux Feedbacks in a New Coupled Large Eddy Model, Journal of Geophysical Research: Atmospheres, 111, https://doi.org/10.1029/2005JD006138, 2006.

Jiang, H., Feingold, G., Cotton, W. R., and Duynkerke, P. G.: Large-Eddy Simulations of Entrainment of Cloud Condensation Nuclei into the Arctic Boundary Layer: May 18, 1998, FIRE/SHEBA Case Study, Journal of Geophysical Research: Atmospheres, 106, 15 113–15 122, https://doi.org/10.1029/2000JD900303, 2001.

Jozef, G. C., Cassano, J. J., Dahlke, S., Dice, M., Cox, C. J., and de Boer, G.: Thermodynamic and kinematic drivers of atmospheric boundary layer stability in the central Arctic during the Multidisciplinary drifting Observatory for the Study of Arctic Climate (MOSAiC), Atmospheric Chemistry and Physics, 23, 13 087–13 106, https://doi.org/10.5194/acp-23-13087-2023, 2023.

Jung, C. H., Yoon, Y. J., Kang, H. J., Gim, Y., Lee, B. Y., Ström, J., Krejci, R., and Tunved, P.: The Seasonal Characteristics of Cloud Condensation Nuclei (CCN) in the Arctic Lower Troposphere, Tellus B: Chemical and Physical Meteorology, 70, 1–13, https://doi.org/10.1080/16000889.2018.1513291, 2018.

Karlsson, L., Krejci, R., Koike, M., Ebell, K., and Zieger, P.: A long-term study of cloud residuals from low-level Arctic clouds, Atmospheric Chemistry and Physics, 21, 8933–8959, https://doi.org/10.5194/acp-21-8933-2021, publisher: Copernicus GmbH, 2021.

Karlsson, L., Baccarini, A., Duplessis, P., Baumgardner, D., Brooks, I. M., Chang, R. Y.-W., Dada, L., Dällenbach, K. R., Heikkinen, L., Krejci, R., Leaitch, W. R., Leck, C., Partridge, D. G., Salter, M. E., Wernli, H., Wheeler, M. J., Schmale, J., and Zieger, P.: Physical and Chemical Properties of Cloud Droplet Residuals and Aerosol Particles During the Arctic Ocean 2018 Expedition, Journal of Geophysical Research: Atmospheres, 127, e2021JD036 383, https://doi.org/10.1029/2021JD036383, _eprint: https://onlinelibrary.wiley.com/doi/pdf/10.1029/2021JD036383, 2022.

Kecorius, S., Vogl, T., Paasonen, P., Lampilahti, J., Rothenberg, D., Wex, H., Zeppenfeld, S., van Pinxteren, M., Hartmann, M., Henning, S., Gong, X., Welti, A., Kulmala, M., Stratmann, F., Herrmann, H., and Wiedensohler, A.: New particle formation and its effect on cloud condensation nuclei abundance in the summer Arctic: a case study in the Fram Strait and Barents Sea, Atmospheric Chemistry and Physics, 19, 14 339–14 364, https://doi.org/10.5194/acp-19-14339-2019, 2019.

Klein, S. A., McCoy, R. B., Morrison, H., Ackerman, A. S., Avramov, A., de Boer, G., Chen, M., Cole, J. N., del Genio, A. D., Falk, M., Foster, M. J., Fridlind, A., Golaz, J. C., Hashino, T., Harrington, J. Y., Hoose, C., Khairoutdinov, M. F., Larson, V. E., Liu, X., Luo, Y., McFarquhar, G. M., Menon, S., Neggers, R. A., Park, S., Poellot, M. R., Schmidt, J. M., Sednev, I., Shipway, B. J., Shupe, M. D., Spangenberg, D. A., Sud, Y. C., Turner, D. D., Veron, D. E., von Salzen, K., Walker, G. K., Wang, Z., Wolf, A. B., Xie, S., Xu, K. M., Yang, F., and Zhang, G.: Intercomparison of Model Simulations of Mixed-Phase Clouds Observed during the ARM Mixed-Phase Arctic Cloud Experiment. I: Single-layer Cloud, Quarterly Journal of the Royal Meteorological Society, 135, 979–1002, https://doi.org/10.1002/qj.416, 2009.

Koike, M., Ukita, J., Ström, J., Tunved, P., Shiobara, M., Vitale, V., Lupi, A., Baumgardner, D., Ritter, C., Hermansen, O., Yamada, K., and Pedersen, C. A.: Year-Round In Situ Measurements of Arctic Low-Level Clouds: Microphysical Properties and Their Relationships With Aerosols, Journal of Geophysical Research: Atmospheres, 124, 1798–1822, https://doi.org/10.1029/2018JD029802, _eprint: https://onlinelibrary.wiley.com/doi/pdf/10.1029/2018JD029802, 2019.

Lonardi, M., Pilz, C., Akansu, E. F., Dahlke, S., Egerer, U., Ehrlich, A., Griesche, H., Heymsfield, A. J., Kirbus, B., Schmitt, C. G., Shupe, M. D., Siebert, H., Wehner, B., and Wendisch, M.: Tethered Balloon-Borne Profile Measurements of Atmospheric Properties in the

Cloudy Atmospheric Boundary Layer over the Arctic Sea Ice during MOSAiC: Overview and First Results, Elementa: Science of the Anthropocene, 10, 000 120, https://doi.org/10.1525/elementa.2021.000120, 2022.

Lonardi, M., Pilz, C., Siebert, H., Ehrlich, A., and Wendisch, M.: Tethered balloon-borne measurements of terrestrial radiation during MOSAiC leg 4 in July 2020, https://doi.org/10.1594/PANGAEA.944200, 2022a.

Lonardi, M., Pilz, C., Siebert, H., Ehrlich, A., and Wendisch, M.: Tethered balloon-borne measurements of liquid cloud water presence during MOSAiC leg 4 in July 2020, https://doi.org/10.1594/PANGAEA.944068, 2022b.

Mauritsen, T., Sedlar, J., Tjernstrom, M., Leck, C., Martin, M., Shupe, M., Sjögren, S., Sierau, B., Persson, P. O. G., and Brooks, I. M.: An Arctic CCN-limited Cloud-Aerosol Regime, Atmospheric Chemistry and Physics, 11, 165–173, 2011.

McCoy, I. L., Bretherton, C. S., Wood, R., Twohy, C. H., Gettelman, A., Bardeen, C. G., and Toohey, D. W.: Influences of Recent Particle Formation on Southern Ocean Aerosol Variability and Low Cloud Properties, Journal of Geophysical Research: Atmospheres, 126, e2020JD033 529, https://doi.org/10.1029/2020JD033529, _eprint: https://onlinelibrary.wiley.com/doi/pdf/10.1029/2020JD033529, 2021.

Meyers, M. P., Walko, R. L., Harrington, J. Y., and Cotton, W. R.: New RAMS Cloud Microphysics Parameterization. Part II: The Two-Moment Scheme, Atmospheric Research, 45, 3–39, https://doi.org/10.1016/S0169-8095(97)00018-5, 1997.

Morrison, H., Pinto, J. O., Curry, J. A., and McFarquhar, G. M.: Sensitivity of Modeled Arctic Mixed-Phase Stratocumulus to Cloud Condensation and Ice Nuclei over Regionally Varying Surface Conditions: SIMULATION OF ARCTIC MIXED-PHASE CLOUDS, J. Geophys. Res., 113, n/a–n/a, https://doi.org/10.1029/2007JD008729, 2008.

Morrison, H., McCoy, R. B., Klein, S. A., Xie, S., Luo, Y., Avramov, A., Chen, M., Cole, J. N. S., Falk, M., Foster, M. J., Del Genio, A. D., Harrington, J. Y., Hoose, C., Khairoutdinov, M. F., Larson, V. E., Liu, X., McFarquhar, G. M., Poellot, M. R., von Salzen, K., Shipway, B. J., Shupe, M. D., Sud, Y. C., Turner, D. D., Veron, D. E., Walker, G. K., Wang, Z., Wolf, A. B., Xu, K.-M., Yang, F., and Zhang, G.: Intercomparison of Model Simulations of Mixed-Phase Clouds Observed during the ARM Mixed-Phase Arctic Cloud Experiment. II: Multilayer Cloud, Quarterly Journal of the Royal Meteorological Society, 135, 1003–1019, https://doi.org/10.1002/qj.415, 2009.

Morrison, H., Zuidema, P., Ackerman, A. S., Avramov, A., De Boer, G., Fan, J., Fridlind, A. M., Hashino, T., Harrington, J. Y., Luo, Y., Ovchinnikov, M., and Shipway, B.: Intercomparison of Cloud Model Simulations of Arctic Mixed-Phase Boundary Layer Clouds Observed during SHEBA/FIRE-ACE, Journal of Advances in Modeling Earth Systems, 3, https://doi.org/10.1029/2011MS000066, 2011.

Morrison, H., De Boer, G., Feingold, G., Harrington, J., Shupe, M. D., and Sulia, K.: Resilience of Persistent Arctic Mixed-Phase Clouds, Nature Geoscience, 5, 11–17, https://doi.org/10.1038/ngeo1332, 2012.

Peng, Y., Lohmann, U., Leaitch, R., Banic, C., and Couture, M.: The Cloud Albedo-Cloud Droplet Effective Radius Relationship for Clean and Polluted Clouds from RACE and FIRE.ACE: EVIDENCE FOR INDIRECT AEROSOL EFFECT, J. Geophys. Res., 107, AAC 1–1–AAC 1–6, https://doi.org/10.1029/2000JD000281, 2002.

Pilz, C., Lonardi, M., Siebert, H., and Wehner, B.: Tethered balloon-borne measurements of aerosol particle microphysics during the MOSAiC expedition from June to July 2020, https://doi.org/10.1594/PANGAEA.943907, 2022a.

Pilz, C., Siebert, H., and Lonardi, M.: Tethered balloon-borne measurements of meteorological parameters during MOSAiC leg 4 in June and July 2020, https://doi.org/10.1594/PANGAEA.952341, 2022b.

Price, R., Baccarini, A., Schmale, J., Zieger, P., Brooks, I. M., Field, P., and Carslaw, K. S.: Late summer transition from a free-tropospheric to boundary layer source of Aitken mode aerosol in the high Arctic, Atmospheric Chemistry and Physics, 23, 2927–2961, https://doi.org/10.5194/acp-23-2927-2023, publisher: Copernicus GmbH, 2023.

Rantanen, M., Karpechko, A. Y., Lipponen, A., Nordling, K., Hyvärinen, O., Ruosteenoja, K., Vihma, T., and Laaksonen, A.: The Arctic Has Warmed Nearly Four Times Faster than the Globe since 1979, Commun Earth Environ, 3, 1–10, https://doi.org/10.1038/s43247-022-00498-3, 2022.

Saleeby, S. M. and Cotton, W. R.: A Large-Droplet Mode and Prognostic Number Concentration of Cloud Droplets in the Colorado State University Regional Atmospheric Modeling System (RAMS). Part I: Module Descriptions and Supercell Test Simulations, Journal of Applied Meteorology, 43, 182–195, https://doi.org/10.1175/1520-0450(2004)043<0182:ALMAPN>2.0.CO;2, 2004.

Saleeby, S. M. and van den Heever, S. C.: Developments in the CSU-RAMS Aerosol Model: Emissions, Nucleation, Regeneration, Deposition, and Radiation, Journal of Applied Meteorology and Climatology, 52, 2601–2622, https://doi.org/10.1175/JAMC-D-12-0312.1, 2013.

Schröder, D., Vihma, T., Kerber, A., and Brümmer, B.: On the parameterization of turbulent surface fluxes over heterogeneous sea ice surfaces, Journal of Geophysical Research: Oceans, 108, https://doi.org/https://doi.org/10.1029/2002JC001385, 2003.

Sedlar, J.: Implications of Limited Liquid Water Path on Static Mixing within Arctic Low-Level Clouds, Journal of Applied Meteorology and Climatology, 53, 2775 – 2789, https://doi.org/https://doi.org/10.1175/JAMC-D-14-0065.1, 2014.

Sedlar, J., Tjernström, M., Mauritsen, T., Shupe, M. D., Brooks, I. M., Persson, P. O. G., Birch, C. E., Leck, C., Sirevaag, A., and Nicolaus, M.: A Transitioning Arctic Surface Energy Budget: The Impacts of Solar Zenith Angle, Surface Albedo and Cloud Radiative Forcing, Clim Dyn, 37, 1643–1660, https://doi.org/10.1007/s00382-010-0937-5, 2011.

Sedlar, J., Shupe, M. D., and Tjernström, M.: On the Relationship between Thermodynamic Structure and Cloud Top, and Its Climate Significance in the Arctic, Journal of Climate, 25, 2374–2393, https://doi.org/10.1175/JCLI-D-11-00186.1, 2012.

Shupe, M. D.: Clouds at Arctic Atmospheric Observatories. Part II: Thermodynamic Phase Characteristics, Journal of Applied Meteorology and Climatology, 50, 645–661, https://doi.org/10.1175/2010JAMC2468.1, 2011.

Shupe, M. D. and Intrieri, J. M.: Cloud Radiative Forcing of the Arctic Surface: The Influence of Cloud Properties, Surface Albedo, and Solar Zenith Angle, Journal of Climate, 17, 616–628, https://doi.org/10.1175/1520-0442(2004)017<0616:CRFOTA>2.0.CO;2, 2004.

Shupe, M. D., Matrosov, S. Y., and Uttal, T.: Arctic Mixed-Phase Cloud Properties Derived from Surface-Based Sensors at SHEBA, Journal of the Atmospheric Sciences, 63, 697–711, https://doi.org/10.1175/JAS3659.1, 2006.

Shupe, M. D., Kollias, P., Persson, P. O. G., and McFarquhar, G. M.: Vertical Motions in Arctic Mixed-Phase Stratiform Clouds, Journal of the Atmospheric Sciences, 65, 1304–1322, https://doi.org/10.1175/2007JAS2479.1, 2008.

Shupe, M. D., Walden, V. P., Eloranta, E., Uttal, T., Campbell, J. R., Starkweather, S. M., and Shiobara, M.: Clouds at Arctic Atmospheric Observatories. Part I: Occurrence and Macrophysical Properties, J. Appl. Meteor. Climatol., 50, 626–644, https://doi.org/10.1175/2010JAMC2467.1, 2011.

Shupe, M. D., Turner, D. D., Walden, V. P., Bennartz, R., Cadeddu, M. P., Castellani, B. B., Cox, C. J., Hudak, D. R., Kulie, M. S., Miller, N. B., Neely, R. R., Neff, W. D., and Rowe, P. M.: High and Dry: New Observations of Tropospheric and Cloud Properties above the Greenland Ice Sheet, Bulletin of the American Meteorological Society, 94, 169–186, https://doi.org/10.1175/BAMS-D-11-00249.1, 2013.

Shupe, M. D., Rex, M., Blomquist, B., Persson, P. O. G., Schmale, J., Uttal, T., Althausen, D., Angot, H., Archer, S., Bariteau, L., Beck, I., Bilberry, J., Bucci, S., Buck, C., Boyer, M., Brasseur, Z., Brooks, I. M., Calmer, R., Cassano, J., Castro, V., Chu, D., Costa, D., Cox, C. J., Creamean, J., Crewell, S., Dahlke, S., Damm, E., de Boer, G., Deckelmann, H., Dethloff, K., Dütsch, M., Ebell, K., Ehrlich, A., Ellis, J., Engelmann, R., Fong, A. A., Frey, M. M., Gallagher, M. R., Ganzeveld, L., Gradinger, R., Graeser, J., Greenamyer, V., Griesche, H., Griffiths, S., Hamilton, J., Heinemann, G., Helmig, D., Herber, A., Heuzé, C., Hofer, J., Houchens, T., Howard, D., Inoue, J., Jacobi, H.-W., Jaiser, R., Jokinen, T., Jourdan, O., Jozef, G., King, W., Kirchgaessner, A., Klingebiel, M., Krassovski, M., Krumpen,

T., Lampert, A., Landing, W., Laurila, T., Lawrence, D., Lonardi, M., Loose, B., Lüpkes, C., Maahn, M., Macke, A., Maslowski, W., Marsay, C., Maturilli, M., Mech, M., Morris, S., Moser, M., Nicolaus, M., Ortega, P., Osborn, J., Pätzold, F., Perovich, D. K., Petäjä, T., Pilz, C., Pirazzini, R., Posman, K., Powers, H., Pratt, K. A., Preußer, A., Quéléver, L., Radenz, M., Rabe, B., Rinke, A., Sachs, T., Schulz, A., Siebert, H., Silva, T., Solomon, A., Sommerfeld, A., Spreen, G., Stephens, M., Stohl, A., Svensson, G., Uin, J., Viegas, J., Voigt, C., von der Gathen, P., Wehner, B., Welker, J. M., Wendisch, M., Werner, M., Xie, Z., and Yue, F.: Overview of the MOSAiC expedition: Atmosphere, Elementa: Science of the Anthropocene, 10, https://doi.org/10.1525/elementa.2021.00060, _eprint: https://online.ucpress.edu/elementa/article-pdf/10/1/00060/780058/elementa.2021.00060.pdf, 2022.

Siegel, K., Neuberger, A., Karlsson, L., Zieger, P., Mattsson, F., Duplessis, P., Dada, L., Daellenbach, K., Schmale, J., Baccarini, A., Krejci, R., Svenningsson, B., Chang, R., Ekman, A. M. L., Riipinen, I., and Mohr, C.: Using Novel Molecular-Level Chemical Composition Observations of High Arctic Organic Aerosol for Predictions of Cloud Condensation Nuclei, Environmental Science & Technology, 56, 13 888–13 899, https://doi.org/10.1021/acs.est.2c02162, publisher: American Chemical Society, 2022.

Silber, I., Fridlind, A. M., Verlinde, J., Russell, L. M., and Ackerman, A. S.: Nonturbulent Liquid-Bearing Polar Clouds: Observed Frequency of Occurrence and Simulated Sensitivity to Gravity Waves, Geophysical Research Letters, 47, e2020GL087 099, https://doi.org/10.1029/2020GL087099, 2020.

Sokolowsky, G. A., Freeman, S. W., and van den Heever, S. C.: Sensitivities of Maritime Tropical Trimodal Convection to Aerosols and Boundary Layer Static Stability, Journal of the Atmospheric Sciences, 79, 2549–2570, https://doi.org/10.1175/JAS-D-21-0260.1, 2022.

Sotiropoulou, G., Sedlar, J., Forbes, R., and Tjernstrom, M.: Summer Arctic Clouds in the ECMWF Forecast Model: An Evaluation of Cloud Parametrization Schemes, Quarterly Journal of the Royal Meteorological Society, 142, 387–400, https://doi.org/10.1002/qj.2658, 2016.

Stephens, G. L., Gabriel, P. M., and Partain, P. T.: Parameterization of Atmospheric Radiative Transfer. Part I: Validity of Simple Models, Journal of the Atmospheric Sciences, 58, 3391–3409, https://doi.org/10.1175/1520-0469(2001)058<3391:POARTP>2.0.CO;2, 2001.

Sterzinger, L. and Igel, A.: Plotting Scripts for Sterzinger and Igel (2023), https://doi.org/10.5281/zenodo.7996595, 2023a.

Sterzinger, L. and Igel, A. L.: Model data for Sterzinger and Igel (2023) "Simulated Idealized Arctic Cloud Sensitivity to Above Cloud CCN Concentrations", https://doi.org/10.5281/zenodo.7986917, 2023b.

Sterzinger, L., Igel, A., and RAMS-Developers: Model source code and namelists for Sterzinger and Igel (2023), https://doi.org/10.5281/zenodo.7991355, 2023.

Sterzinger, L. J., Sedlar, J., Guy, H., Neely III, R. R., and Igel, A. L.: Do Arctic Mixed-Phase Clouds Sometimes Dissipate Due to Insufficient Aerosol? Evidence from Comparisons between Observations and Idealized Simulations, Atmospheric Chemistry and Physics, 22, 8973–8988, https://doi.org/10.5194/acp-22-8973-2022, 2022.

Stevens, R. G., Loewe, K., Dearden, C., Dimitrelos, A., Possner, A., Eirund, G. K., Raatikainen, T., Hill, A. A., Shipway, B. J., Wilkinson, J., Romakkaniemi, S., Tonttila, J., Laaksonen, A., Korhonen, H., Connolly, P., Lohmann, U., Hoose, C., Ekman, A. M., Carslaw, K. S., and Field, P. R.: A Model Intercomparison of CCN-limited Tenuous Clouds in the High Arctic, Atmospheric Chemistry and Physics, 18, 11 041–11 071, https://doi.org/10.5194/acp-18-11041-2018, 2018.

Taylor, P. C., Cai, M., Hu, A., Meehl, J., Washington, W., and Zhang, G. J.: A Decomposition of Feedback Contributions to Polar Warming Amplification, Journal of Climate, 26, 7023–7043, https://doi.org/10.1175/JCLI-D-12-00696.1, 2013.

Verlinde, J., Harrington, J. Y., McFarquhar, G. M., Yannuzzi, V. T., Avramov, A., Greenberg, S., Johnson, N., Zhang, G., Poellot, M. R., Mather, J. H., Turner, D. D., Eloranta, E. W., Zak, B. D., Prenni, A. J., Daniel, J. S., Kok, G. L., Tobin, D. C., Holz, R., Sassen, K., Spangenberg, D., Minnis, P., Tooman, T. P., Ivey, M. D., Richardson, S. J., Bahrmann, C. P., Shupe, M., DeMott, P. J., Heymsfield, A. J.,

and Schofield, R.: The Mixed-Phase Arctic Cloud Experiment, Bull. Amer. Meteor. Soc., 88, 205–222, https://doi.org/10.1175/BAMS-88-2-205, 2007.

Walko, R., Cotton, W., Meyers, M., and Harrington, J.: New RAMS Cloud Microphysics Parameterization Part I: The Single-Moment Scheme, Atmospheric Research, 38, 29–62, https://doi.org/10.1016/0169-8095(94)00087-T, 1995.

Willis, M. D., Burkart, J., Thomas, J. L., Köllner, F., Schneider, J., Bozem, H., Hoor, P. M., Aliabadi, A. A., Schulz, H., Herber, A. B., Leaitch, W. R., and Abbatt, J. P. D.: Growth of nucleation mode particles in the summertime Arctic: a case study, Atmospheric Chemistry and Physics, 16, 7663–7679, https://doi.org/10.5194/acp-16-7663-2016, publisher: Copernicus GmbH, 2016.

Wood, R.: Drizzle in Stratiform Boundary Layer Clouds. Part I: Vertical and Horizontal Structure, Journal of the Atmospheric Sciences, 62, 3011–3033, https://doi.org/10.1175/JAS3529.1, 2005a.

Wood, R.: Drizzle in Stratiform Boundary Layer Clouds. Part II: Microphysical Aspects, Journal of the Atmospheric Sciences, 62, 3034–3050, https://doi.org/10.1175/JAS3530.1, 2005b.

Wyant, M. C., Bretherton, C. S., Wood, R., Blossey, P. N., and McCoy, I. L.: High Free-Tropospheric Aitken-Mode Aerosol Concentrations Buffer Cloud Droplet Concentrations in Large-Eddy Simulations of Precipitating Stratocumulus, Journal of Advances in Modeling Earth Systems, 14, e2021MS002 930, https://doi.org/10.1029/2021MS002930, _eprint: https://onlinelibrary.wiley.com/doi/pdf/10.1029/2021MS002930, 2022.

Wylie, D. P. and Hudson, J. G.: Effects of Long-Range Transport and Clouds on Cloud Condensation Nuclei in the Springtime Arctic, Journal of Geophysical Research: Atmospheres, 107, AAC 13–1–AAC 13–11, https://doi.org/10.1029/2001JD000759, 2002.